

# Near Infrared Observations of the Extremely Red Object

## CL 0939+4713 B : An Old Galaxy at $z \sim 1.58$ ? <sup>1</sup>

B.T. Soifer<sup>2,3</sup>, K. Matthews<sup>2</sup>, G. Neugebauer<sup>2</sup>, L. Armus<sup>3</sup>, J. G. Cohen<sup>4</sup>, S.E. Persson<sup>5</sup>, I.  
Smail<sup>6</sup>

Received 1999 August;    accepted \_\_\_\_\_

---

<sup>1</sup>Based on observations obtained at the W.M. Keck Observatory, which is operated as a scientific partnership among the California Institute of Technology, the University of California and the National Aeronautics and Space Administration

<sup>2</sup>Palomar Observatory, 320-47, Caltech, Pasadena, CA 91125

<sup>3</sup>SIRTF Science Center, 310-6, Caltech, Pasadena, CA 91125

<sup>4</sup>Palomar Observatory, 105-24, Caltech, Pasadena, CA 91125

<sup>5</sup>Carnegie Observatories, 813 Santa Barbara St. Pasadena, CA 91101

<sup>6</sup>Department of Physics, University of Durham, South Road, Durham DH1 3LE, UK

## ABSTRACT

Near infrared imaging and spectroscopic observations of the extremely red object ( $R - K \sim 7$  mag) CL 0939+4713 B have been obtained with the Near Infrared Camera on the Keck I Telescope of the W. M. Keck Observatory. The imaging shows a slightly elongated structure, while the spectroscopy shows a continuum break that allows us to determine the redshift of  $z = 1.58 + 0.01 / - 0.03$  for this system. The fits of a range of models to the infrared spectrum suggests that it is predominantly an old ( $> 10^9$  yrs) stellar system that suffers little extinction, while the measured  $R$  and  $I$  magnitudes suggests an age of  $\sim 3 \times 10^8$  years. The limit on the equivalent width of any emission line in the infrared spectrum argues that CL 0939+4713 B is not an actively star forming galaxy. This system, though similar in  $R - K$  color to HR 10 [also known as J1645+46] (Dey et al. 1999), is much different in morphology and emission line strengths, demonstrating the heterogeneity of extremely red extragalactic objects (EROs) selected on the basis of large values of  $R - K$ .

*Subject headings:* Galaxies: distances and redshifts; evolution

## 1. Introduction

Over the last decade several groups (Elston, Rieke & Rieke, 1988,1989, Eisenhardt & Dickinson, 1992, McCarthy, Persson & West, 1992, Persson, McCarthy, Dressler & Matthews, 1993, Hu & Ridgway, 1994, Dey, Spinrad & Dickinson, 1995, Djorgovski et al. 1995, Barger et al. 1999) have reported finding a class of extremely red objects (EROs) with  $R - K > 6$  mag that are reasonably bright ( $K < 19$  mag) and are relatively frequent (surface densities  $\sim 0.01/\text{sq arcmin}$  at  $K < 18$  mag, Hu & Ridgway, Thompson et al. 1999).

The earliest studies suggested that these systems might be at extremely high redshifts (Elston, Rieke & Rieke 1988), but this has not been borne out. Recent work has shown that these systems have spectral energy distributions in the visible and near infrared consistent with elliptical galaxies or very dusty galaxies at  $z > 1$  (Persson et al 1993, Hu & Ridgway, 1994, Trentham, Kormendy and Sanders, 1999). Recently Graham & Dey (1996) have reported imaging and spectroscopy of one of the brightest of these red objects, HR 10, discovered by Hu & Ridgway. Graham and Dey report the detection of a spectral feature at  $1.6\mu\text{m}$  which they associate with  $\text{H}\alpha$  at a redshift  $z=1.44$ . They further suggest that the morphology of this system is consistent with an interacting galaxy system, suggesting that this is a dusty starburst galaxy or AGN. Dey et al. (1999) confirm the redshift of HR 10 with the detection of  $[\text{OII}]3727\text{\AA}$ . Both Dey et al. and Cimatti et al. (1998) report the detection of HR 10 at submillimeter wavelengths, supporting the suggestion of its being a dusty, interacting galaxy. Smail et al. (1999) have also suggested that up to half of the EROs could be associated with submillimeter sources detected in SCUBA surveys.

Understanding the nature of EROs, or even whether they represent a homogeneous class, is important for several reasons. If these are indeed starburst/AGN systems at  $z > 1$ , they could be the high redshift analogs of the ultraluminous infrared galaxies seen locally (e.g. Soifer et al. 1984, Sanders et al 1988, Trentham, Kormendy and Sanders, 1999 ). If

powered by hot, young stars, such systems would have star formation rates greater than that found for most of the young galaxies at  $z \geq 3$  found by Steidel et al. (1996). Alternatively if they are distant passively evolving elliptical galaxies, then the determination of their ages might well place significant constraints on the formation epoch of massive galaxies.

As part of a program to study the nature of these objects we have undertaken near infrared spectroscopy of one of the brightest of these objects on the Keck I Telescope of the W.M. Keck Observatory. In this paper we report spectroscopy and imaging for CL 0939+4713 B, an object serendipitously found by Persson et al. (1993) in the infrared in the field of a rich cluster of galaxies at  $z=0.41$  (Dressler and Gunn, 1992) and referred to by them as  $9\alpha\beta$  B. It is non-stellar, and located  $\simeq 4''$  southwest of galaxy 174 in the cluster (Dressler and Gunn). Persson et al. reported a  $K$  magnitude of 18.3 mag and  $r - K > 7.4$  mag. Assuming a passively evolving stellar population, Persson et al. estimated a redshift of 1.8 for CL 0939+4713 B and an age of  $3 \times 10^9$  yr, by fitting their photometry at  $r, i, J, H$  and  $K$  to Bruzual (1985) models. The grism observations reported here allow us to search for emission lines such as those found in the spectrum of HR 10, as well as to directly measure any continuum in the spectrum. Throughout this paper we adopt  $H_o = 50$  km  $s^{-1} Mpc^{-1}$  and  $q_o = 0.5$  (and  $\Lambda = 0$ ).

## 2. Observations and Data Reduction

Photometric and grism observations of CL 0939+4713 B were made on 1997 March 31 using the Near Infrared Camera (NIRC; Matthews and Soifer, 1994) on the Keck I Telescope. The array has  $256 \times 256$  pixels and a scale of  $0.15''/\text{pixel}$ . Photometry at  $J(1.27 \mu m)$ ,  $H(1.65 \mu m)$  and  $K(2.2 \mu m)$  was obtained in seeing with FWHM  $\sim 0.4''$ ; the data were calibrated by reference to calibration stars of Persson et al.(1998).

The final  $K$ -band image shown in Figure 1 was created by combining 15 individual frames of 12 seconds each, taken both before and after the spectral data. The telescope was moved 5-10'' between individual frames, and sky and flat field images were constructed from the data themselves, after masking out bright sources in the field. Although there are no obvious point sources on the image of CL 0939+4713 B itself, the seeing at the time of the observations was estimated to have a FWHM  $\simeq 0.4''$ , measured from standard stars observed immediately before the data were taken.

Low resolution spectra were obtained that span the range  $1 - 2.4 \mu\text{m}$  in two wavelength settings. For the wavelength range  $1.0 - 1.6 \mu\text{m}$  4500 seconds of observations were made, while 7800 seconds of observations were made for the range  $1.6 - 2.4 \mu\text{m}$ ; individual observations were  $\sim 300$  sec in duration. The slit was 4.5 pixels ( $\sim 0.68''$ ) wide and aligned essentially north-south so the bright galaxy to the south was included in most spectra. The object was moved to five positions along the slit for successive integrations.

The data were processed in a conventional manner. The spectra were corrected for atmospheric features by dividing the spectra of CL 0939+4713 B by that of a G6V star observed on the same night at similar air mass. The spectrum of the G6V star closely approximates that of a blackbody of temperature  $5600K$  at the spectral resolution of the observations and so was assumed to follow the blackbody spectrum. The infrared spectrum and R band photometry were put on a common absolute scale by integrating the infrared spectra over the appropriate wavelength bands and scaling the spectral flux densities to correspond to the photometry in a  $3''$  diameter beam. The infrared data were boxcar smoothed to 2 pixels, i.e.  $\Delta\lambda = 0.0135 \mu\text{m}$ , the spectral resolution corresponding to half the slit width.

In addition to the near infrared observations, images of CL 0939+4713 B were taken using the Low Resolution Imaging Spectrograph (LRIS; Oke et al. 1995) on the Keck II

Telescope. Three 600 second images, slightly offset in pointing location between images, were taken through an  $R$  filter in 1998 March. The seeing on the summed image was  $\text{FWHM} \simeq 0.9''$ . Eighteen 200 second images with slight positional offsets were taken in the  $I$  filter on 1998 November 01 (see Smail et al. 1999). The night was photometric and the total integration time was 3,600 sec; the seeing was  $0.65''$  FWHM. The data for both images were reduced using standard techniques. The photometry was calibrated to the standard system of Landolt (1992).

### 3. Results

The  $R$  and  $K$  images of CL 0939+4713 B are shown in Figure 1 while Table 1 reports the photometry for the source. The  $K$  image shows that CL 0939+4713 B is resolved, having a bright core with a clear elongation in the east west direction. The  $K$  magnitude of CL 0939+4713 B from the Keck imaging is  $18.16 \pm 0.06$  mag in a  $3''$  diameter beam. To determine whether this value is affected by the presence of the nearby brighter galaxy (galaxy 174), the bright galaxy was subtracted from the image by rotating the image by  $180^\circ$  about the center of galaxy 174 and subtracting it from the original image. This successfully eliminated galaxy 174, while preserving the other objects in the image. The  $K$  magnitude of CL 0939+4713 B measured in the image where galaxy 174 was eliminated is  $18.26 \pm 0.10$  mag. Our conclusion from this is that the two measurements are consistent within the uncertainties and galaxy 174 does not significantly affect the measurement of CL 0939+4713 B at  $K$  in a  $3''$  diameter beam. The  $K$  measurement of Persson et al. (1993) is consistent with the value reported here.

The spectrum of CL 0939+4713 B, plotted vs. observed wavelength from  $1.0 - 2.4 \mu\text{m}$ , is shown in Figure 2. The flux scale of Figures 2 and 3 is set so that the flux level in the spectrum agrees with the average of the Keck photometry at  $J$ ,  $H$  and  $K$  as presented in

Table 1. Because the spectral standard that was used is not calibrated photometrically, there is no independent calibration of the spectrophotometry. The spectrum is comparatively flat for wavelengths  $\lambda > 1.2\,\mu\text{m}$  and drops rapidly below this wavelength. There are no strong narrow emission features in the spectrum, and the only strong continuum feature is the apparent change of slope at  $1.2\,\mu\text{m}$ .

In the  $R$  image the object is also resolved, with a measured FWHM of  $1.27''$ . The original  $r$  magnitude for CL 0939+4713 B reported by Persson et al. (1993) was  $r > 25.7$  mag, based on a non-detection of the source in the  $r$  image of the field. The Keck  $R$  image detects the source with a measured magnitude of 25.57 mag in a  $1.3''$  diameter beam. The aperture correction to a  $3''$  diameter was determined to be 0.44 mag (with substantial scatter  $\sim 0.4$  mag) using objects of similar brightness in the same image. This leads to a total  $R$  magnitude of  $25.13 +0.5/-0.3$  mag. Uncertainties in the  $R$  magnitude in addition to the aperture correction arise because of the proximity, within  $\sim 4''$ , of the much brighter galaxy (galaxy 174 in the cluster; Figure 1) to the northeast.

The  $R$  magnitude reported here is somewhat brighter than the original limit  $r > 25.7$  mag of Persson et al.(1993). The measurement at  $R$  and limit at  $r$  are entirely consistent with the transformation between  $r$  and  $R$  magnitudes given by Kent (1985). The color derived from the Keck data is  $R - K = 7 \pm 0.5$  mag, and is dominated by the uncertainty in the  $R$  magnitude.

There are no galaxies apparent closer than  $4''$  to CL 0939+4713 B , although CL 0939+4713 A, as reported by Persson et al.(1993), is  $\sim 7''$  away and has an  $r - K$  color of 6.2 mag. The Keck observations give an  $R$  magnitude of 24.75 mag for CL 0939+4713 A, in excellent agreement with the  $r$  magnitude of 24.7 mag from Persson et al.

CL 0939+4713 B is very clearly resolved in the  $I$  image with a magnitude in a  $2''$  diameter beam of  $I = 23.26 \pm 0.07$  mag. The aperture correction to a  $3''$  diameter beam

is  $\sim -0.1$  mag yielding an  $I$  magnitude in a  $3''$  diameter beam of  $I = 23.16 \pm 0.15$  mag. The measured  $I$  magnitude leads to a flux density a factor of  $\sim 3$  greater than the flux density determined from the  $i$  magnitude of Persson et al. (1993). The extended long wavelength spectral response in the  $I$  measurement can account for some, but not all, of this discrepancy.

The LRIS  $R$  and  $I$ -band photometry is included in Figure 3 and is discussed below.

#### 4. Discussion

The nature of the high Galactic latitude extremely red objects is still highly uncertain. Spectral energy distributions of old stellar populations, and young, reddened galaxies are consistent with the broad band observations for many of the extremely red objects, and more detailed observations are required to distinguish between these alternatives. In the case of HR 10 (Hu and Ridgway, 1994), the detection of emission lines and a submillimeter continuum (Graham and Dey, 1996, Cimatti et al. 1998, Dey et al. 1999) argue convincingly that this is a comparatively “young” galaxy whose colors are substantially affected by reddening.

The observed  $R - K$  color of CL 0939+4713 B places it among the extremely red objects found in field surveys at  $K$  (Hu and Ridgway 1994, Cohen et al. 1998, Barger et al. 1999, Thompson et al. 1999). The spectral energy distribution of Figure 3 allows us to place constraints on the redshift, the reddening, and the evolutionary state of this galaxy. We first provide a qualitative view, considering two extreme states, a very young and a very old galaxy, and then introduce galaxy models to deduce quantitative results. We consider the possibility of dust in the nearby galaxy 174 affecting CL 0939+4713 B to be most unlikely. The projected separation of the two objects,  $\sim 30$  kpc at  $z=0.41$  is very



large, so significant dust would have to present at a very large distance from the center of that galaxy. Secondly, the low redshift ( $z=0.41$ ) of galaxy 174 means that any reddening of the observed infrared light in CL 0939+4713 B due to the intervening galaxy would be affecting wavelengths not substantially different from the observed wavelengths. This would require substantially more dust to produce an observable effect than would be the case if the dust is associated with the (presumably) much higher redshift source CL 0939+4713 B.

If the galaxy is very old, the integrated light is dominated by G and K stars. The apparent break near  $1.2\mu\text{m}$  then must be the  $4000\text{\AA}$  break. It cannot be the  $2800\text{\AA}$  break, as this would be weaker than the  $4000\text{\AA}$  break, which would then lie at  $\sim 1.7\mu\text{m}$ , and there is no sign of this feature in the spectral energy distribution (SED) of Figure 3. As described below, we consider the possibility of the break being due to the Lyman limit being most unlikely. The redshift is thereby constrained to lie near  $z=2$ . The flat continuum observed in the near infrared is then the Paschen continuum of G/K stars, and since the observed continuum is not very red itself, the reddening must then be small.

If the galaxy is very young, there is no natural strong break in the spectrum of hot stars except the Lyman limit. We rule out a Lyman limit break because of the detection of the galaxy at  $R$  and  $I$ , as well as considerations of plausible luminosities. The break and apparent slope must then be attributed to the effects of reddening. The spectra of local starbursts are smooth (Schmitt et al. 1997) and the reddening is approximately inversely proportional to wavelength so that there is no way to reproduce the strong break seen at  $1.2\mu\text{m}$  in the spectrum. In this case, there is no qualitative match to the observed SED with a normal reddening curve for any choice of redshift.

To make this comparison more quantitative, we fit the observed infrared spectrum with the population synthesis models of Bruzual and Charlot (1993, 1996). Because the data are not of high signal to noise ratio, there is limited information that can be derived from

model fitting. We fit instantaneous burst models of metal abundances  $Z = Z_{\odot}$ ,  $Z = 0.2Z_{\odot}$  and a range of ages. For each age model, the redshift and reddening (using the reddening law from Gordon and Clayton, 1998) were varied to minimize the  $\chi^2$  of the fit. The models were fit only to the near-infrared data because the  $R$  and  $I$  data were qualitatively and quantitatively different from the grism data. The consistency of the  $R$  and  $I$  data with the various model fits was, however, checked. The results of the fits are given in Table 2.

The redshift of CL 0939+4713 B, determined in this manner, was comparatively insensitive to the metal abundance, age and reddening of the model and was established primarily by fitting the drop in observed flux below  $1.2\mu\text{m}$  to the break in the continuum for the model. Formally the best fit redshift is consistently around 1.58, although the minimum reduced  $\chi^2$  was 2.5 or greater. For a given model, the  $\chi^2$  increases substantially at  $z < 1.55$  and  $z > 1.59$ , so we take  $1.55 < z < 1.59$ , or  $z = 1.58 + 0.01 / - 0.03$  as the result of our fitting. Persson et al. (1993) determined a redshift of 1.8 for this object based on fitting their  $r, i, J, H$  and  $K$  data to Bruzual (1985) models. Presumably the difference between the photometric redshift and that determined here is fitting the  $4000\text{\AA}$  break to the steep slope observed at  $\lambda < 1.2\mu\text{m}$  in the spectroscopic data presented here.

While none of the models provides a statistically acceptable fit, the  $\chi^2$  parameter provides a quantitative measure consistent with the visual comparison of the relative goodness of fit of the different models. The older models with solar metal abundances,  $Z = Z_{\odot}$ , provide better fits to the data than do the models with abundances  $Z = 0.2Z_{\odot}$ . The break at  $1.2\mu\text{m}$  is quite strong, and best fit by old stellar populations with solar abundances. Effects that increase the restframe flux shortward of rest wavelength  $\sim 4000\text{\AA}$  such as decreased UV opacity due to lower metallicity or the presence of hot stars, give lower quality fits to the data. The results of the fits to the  $Z = Z_{\odot}$  models are shown Figure 3. In Figure 3 we have plotted the best fit models in the observed frame with

$Z = Z_{\odot}$  for ages of  $10^7, 10^8, 2.9 \times 10^8, 10^9$  and  $10^{10}$  yrs. For the models with ages of  $10^9$  and  $10^{10}$  yrs, the overall continuum shape, both the slope at  $\lambda > 1.2\mu\text{m}$  and the steep drop to shorter wavelengths, are well fit with a stellar continuum and modest reddening. In the two younger stellar population models, the slope of the continuum is set predominantly by the reddening, with the redshift of the Balmer discontinuity then adjusted accordingly. The younger age population models produce too much flux in the UV to match both the continuum at  $\lambda > 1.2\mu\text{m}$  and the drop to shorter wavelengths with the smooth reddening curve adopted. The adoption of a different reddening law, such as that of Calzetti (1997), does not modify these conclusions, only the quantitative amount of reddening, since over the wavelength range appropriate to the fit the reddening is a power law  $A_v \sim \lambda^{-1}$  with no unique spectral features.

The models with a single initial burst of star formation lead to the reddest colors for a given age, and thereby lead to the least reddening required to fit a given age stellar population to the observed spectrum. We use the model fits to constrain the formation redshift of CL 0939+4713 B. Because a given age single burst model is redder than any model with ongoing star formation, this model fit to the data will be the youngest population model consistent with the data. Thus, the single burst models are the most “conservative” fits to the observed spectrum of Figure 3, i.e. the youngest and least reddened, and hence require the lowest formation redshift to fit the data. More complex models, e.g. exponentially decaying burst models, would require star formation to have begun at a larger redshift.

We have included the  $R$  and  $I$  photometric fluxes in Figure 3. Because of the wide bandpass of the two LRIS filters, and the wide range in SEDs between the calibrating stars and the models, care was taken to properly account for the shift in effective wavelength in the different models, ie. color correcting the predicted fluxes to the scale set by the

standards measurements. Because the range of colors of standards is much less than the colors of the ERO, this by necessity was done by calculation rather than observations.

The models with  $t \geq 10^9$ yr provide better fits to the infrared spectrum than do the younger models. At wavelengths  $\leq 1.2\mu\text{m}$  the older models follow the observed drop in flux, while the younger models do not. The observed  $R$ -band flux is consistent with the flux calculated for the  $10^9$  yr age models. The models with ages of  $10^8$  and  $10^{10}$  years are also acceptable fits to the observed  $R$ -band flux. Clearly any single burst model of age substantially  $< 10^8$  yrs produces significantly more flux than observed. Including the  $I$  data suggest that the age is less than that suggested by the infrared data. If the model is constrained to pass through the measured  $R$  and  $I$  fluxes, a model with an age of  $2.9 \times 10^8$  years agrees with the infrared data, although the quality of the fit to the infrared data alone is significantly worse than for the older models.

If  $z = 1.58$  for CL 0939+4713 B the rest-frame absolute  $B$  magnitude is  $M_B = -22.3$  mag, uncorrected for extinction. Mobasher, Sharples and Ellis (1993) find  $M_B^* \simeq -21.3$  mag for nearby galaxies, so that the luminosity of CL 0939+4713 B is  $\simeq 2.5L^*$ , a reasonable value for a massive galaxy at this redshift. A significant uncertainty in the luminosity calculation is whether CL 0939+4713 B suffers significant magnification due to its presence behind a foreground rich cluster (Dressler and Gunn, 1992). While analysis of the magnification due to the foreground cluster is beyond the scope of this paper, Smail, et al. (1998) suggest a median (flux) magnification factor in the line-of-sight to rich clusters including 0939+4713 (but somewhat closer to the center of the cluster than represented by CL 0939+4713 B) of a factor of 2.5. Such a magnification factor would serve to reduce the luminosity of CL 0939+4713 B to a present day  $L^*$  galaxy if there is no significant extinction affecting the observed flux.

As noted above, there is no evidence for emission lines in the spectrum of

CL 0939+4713 B. The  $3\sigma$  limit on the equivalent width of any emission line in the spectrum of Figure 2 is  $0.004\mu\text{m}$ . If those portions of the spectrum most affected by the atmosphere and filter cut-offs are removed from the calculation of the standard deviation of the flat continuum, the  $3\sigma$  equivalent width is decreased to  $0.003\mu\text{m}$ . This corresponds to a limit on the equivalent width of any emission line in the rest frame spectrum from  $0.4 - 1.0\mu\text{m}$  of  $12\text{\AA}$  if the redshift is given by our fit to the continuum. In particular, at a redshift of 1.55-1.60, the  $3\sigma$  limit on the rest equivalent width of  $\text{H}\alpha + [\text{NII}]$  is  $< 12\text{\AA}$ . This limit is more than a factor of 10 lower than the strength of the  $\text{H}\alpha + [\text{NII}]$  line found in the near infrared spectrum of HR 10 by Dey et al. (1999). We can immediately say that the emission line strengths of HR 10 and CL 0939+4713 B are very different if our determination of the redshift of CL 0939+4713 B is correct.

If we assume that the equivalent width of  $\text{H}\alpha$  is 0.75 of the equivalent width of  $\text{H}\alpha + [\text{NII}]$  (Kennicutt, 1983), this corresponds to a limit of  $< 9\text{\AA}$  on the rest equivalent width of  $\text{H}\alpha$ . We convert the equivalent width to a line luminosity using the observed magnitude and a redshift  $z \simeq 1.6$  (and assuming no magnification); using the relationship between  $\text{H}\alpha$  luminosity and star formation rate from Kennicutt, this corresponds to a limit of  $< 9M_{\odot}\text{yr}^{-1}$  on the star forming rate of CL 0939+4713 B. In terms of equivalent width, the limit of  $< 12\text{\AA}$  on the equivalent width of  $\text{H}\alpha + [\text{NII}]$  would place CL 0939+4713 B among the less active disk galaxies in the local neighborhood (Kennicutt) or the least active of infrared selected galaxies (Veilleux et al. 1995). The limit on the  $\text{H}\alpha$  equivalent width is consistent with continuous star formation lasting for more than  $3 \times 10^8$  yrs based on the models of Leitherer and Heckman (1995). Thus there is reasonably compelling evidence that CL 0939+4713 B is not a reddened, young star forming galaxy, as is the case for HR 10.

Cohen, et al. (1999) have suggested that the objects found in the Caltech Faint Galaxy

Redshift Survey with  $R - K > 5$  mag are old systems that are not reddened, consistent with the interpretation of Spinrad et al. (1997). The identification of CL 0939+4713 B as a distant galaxy whose SED is not significantly affected by dust obscuration places it in the category of potentially old galaxies at high redshift.

HR 10 and CL 0939+4713 B have quite similar visual - infrared colors. The detailed properties, i.e. morphology and infrared spectra of these two systems are very different, leading to very different pictures of the underlying galaxies. This suggests that the objects selected on the basis of red colors between visual and near infrared wavelengths (EROs) represent a heterogeneous group, and a much larger sample of these systems must be carefully studied to establish their context in the high redshift universe.

We thank W. Harrision for assistance with the infrared observations, Rob Ivison, Len Cowie and Amy Barger for obtaining the  $I$  image, Marcin Sawicki for helpful discussions and Dave Thompson for a careful reading of the manuscript and several important suggestions. The W.M. Keck Observatory is operated as a scientific partnership between the California Institute of Technology, the University of California and the National Aeronautics and Space Administration. It was made possible by the generous financial support of the W.M. Keck Foundation. Infrared astronomy at Caltech is supported by grants from the NSF and NASA. This research has made use of the NASA/IPAC Extragalactic Database which is operated by the Jet Propulsion Laboratory, Caltech, under contract with NASA.

Table 1: Photometry of CL 0939+4713 B

Filter	mag (3'' diam. beam)	Ref
R	$25.13 \pm 0.5 / -0.3$	(1)
r	$> 25.7 \text{ } 3\sigma$	(2)
i	$25.19 \pm 0.4$	(2)
I	$23.16 \pm 0.15$	(1)
J	$20.48 \pm 0.4$	(2)
J	$20.36 \pm 0.37 / -0.28$	(1)
H	$19.50 \pm 0.3$	(2)
H	$18.98 \pm 0.20$	(1)
K	$18.26 \pm 0.10$	(2)
K	$18.16 \pm 0.06$	(1)

---

(1) This work

(2) Persson et al. (1993)

Table 2: Redshift and Reddening Resulting from the Best Fits of Stellar Population Models to the Infrared Spectrum of CL 0939+4713 B

Age	z	$Z_{\odot}$		$0.2Z_{\odot}$	
		$A_v$	z	$A_v$	
		mag		mag	
$1 \times 10^{10}$	1.578	0.1	1.578	0.5	
$1 \times 10^9$	1.582	1.1	1.582	1.4	
$2.9 \times 10^8$	1.588	1.9	1.586	1.9	
$1 \times 10^8$	1.589	2.3	1.582	2.2	
$1 \times 10^7$	1.589	1.8	1.586	2.4	



## REFERENCES

- Barger, A., Cowie, L.L., Trentham, N., Fulton, E., Hu, E.M., Songaila, A., and Hall, D. 1999, AJ, 117, 102
- Bruzual, G 1985, RMxAA, 10, 55
- Bruzual, G. and Chalot, S. 1993, ApJ, 405, 538
- Bruzual, G. and Chalot, S. 1996, in preparation
- Calzetti, D. 199, AJ, 113, 162
- Cimatti, A., Andreani, P., Röttgering, H. and Tilanus, R. 1998, Nature, 392, 895
- Cohen, J.G., Blandford, R.D., Hogg, D.W., Pahre, M.A., and Shopbell, P.L., 1999, ApJ, 512, 30
- Dey, A., Graham, J.R., Ivison, R.J., Smail, I. and Wright, G.S. 1999, astro-ph 9902044
- Dey, A., Spinrad, H. and Dickinson, M. 1995, ApJ, 440, 515
- Djorgovski, S., et al., 1995, ApJ, 438, L13
- Dressler, A and Gunn, J.E., 1992, ApJS, 78,1
- Eisenhardt, P. and Dickinson, M. 1992, ApJ, 399, L47
- Elston, R., Rieke , G.H., and Rieke, M. 1988, ApJ, 331, L77
- Elston, R., Rieke , M., and Rieke, G.H. 1989, ApJ, 341, 80
- Gordon K.D. and Clayton, G.C. 1998, ApJ, 500, 816
- Graham, J.R. and Dey, A. 1996, ApJ, 471, 720

- Hu, E. and Ridgway, S. 1994, AJ, 107, 1303
- Joint IRAS Science Team, 1989, IRAS Point Source Catalog, Version 2 (Washington, DC, US Government Printing Office)
- Kennicutt, R.C. 1983, ApJ, 272, 54
- Kent, S.M. 1985, PASP, 97, 165
- Landolt, A. 1992, AJ, 104, 340
- Leitherer, C. and Heckman, T.M. 1995, ApJS, 96, 9
- Matthews, K. and Soifer, B.T. 1994, *Infrared Astronomy with Arrays: the Next Generation*, I. McLean ed. (Dordrecht: Kluwer Academic Publishers), p.239
- McCarthy, P., Persson, S.E. and West, 1992, ApJ, 386, 52
- Mobasher, B., Sharples, R.M. and Ellis, R.S. 1993, MNRAS, 263,560
- Oke, J.B. et al. 1995, PASP, 107, 307
- Persson, S. E., Murphy, D. C., Krzeminski, W., Roth, M. and Rieke, M. 1998, AJ, 116, 2475
- Persson, S.E., McCarthy, P., Dressler, A., and Matthews, K. 1993, in *the Evolution of Galaxies and their Environments*, M. Shull and Thronson, H. eds. (NASA Tech. Report, GPO), p.78
- Sanders, D.B., Soifer, B.T., Elias, J.H., Madore, B.F., Matthews, K., Neugebauer, G. and Scoville, N.Z. 1988, ApJ, 325, 74
- Schmitt, H.R., Kinney, A.L., Calzetti, D. and Storchi-Bergmann, T. 1997, AJ, 114, 592
- Smail, I., Ivison, R., Blaine, A. and Kneib, J-P. 1998, astro-ph 9810281

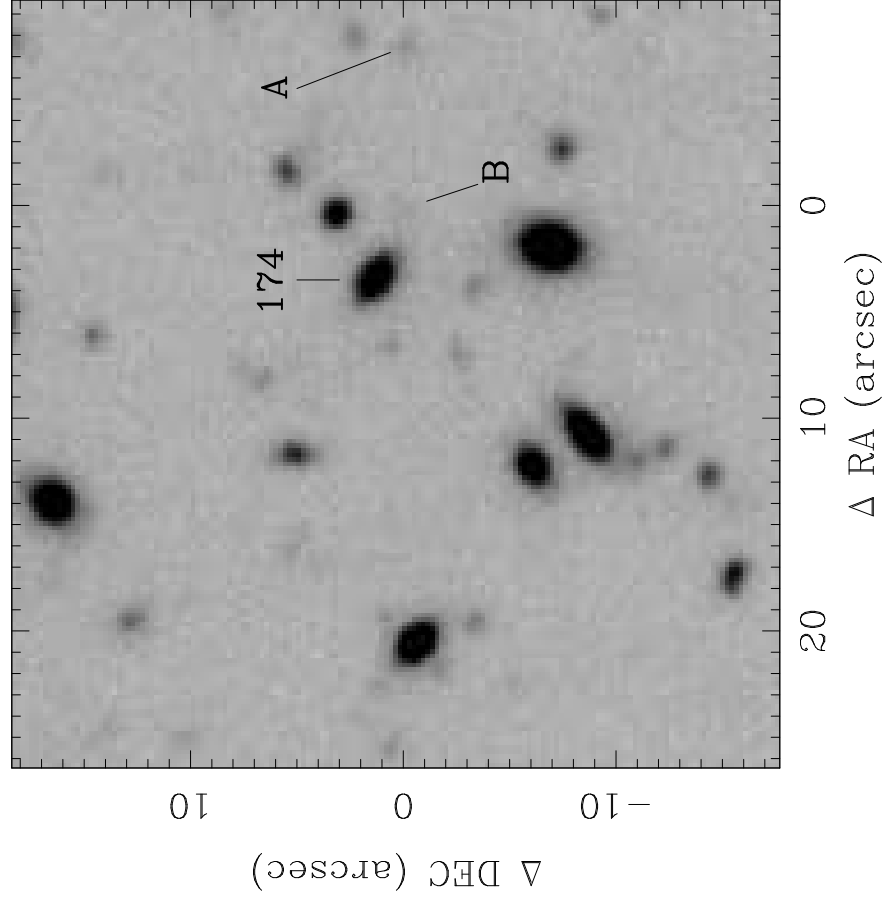
- Smail, I., Ivison, R., Kneib, J-P., Cowie, L.L., Blaine, A.W., Barger, A.J., Owen, F.N. and Morrison, G.E. 1999, astro-ph 9905246, MNRAS(in press)
- Spinrad, H., Dey, A., Stern, D., Dunlop, J.S., Peacock, J.A., Jimenez, R., and Windhorst, R.A., 1997, ApJ, 484, 581
- Soifer, B.T., et al 1984, ApJ, 283, L1
- Steidel, C.C., Giavalisco, M., Pettini, M., Dickinson, M. and Adelberger, K.L. 1996a, ApJ, 462, L17
- Thompson, D.J. et al. 1999, ApJ, in press (astro-ph/9907216)
- Trentham, N., Kormendy, J. and Sanders, D. 1999, AJ, 117, 1152
- Veilleux, S., Kim, D.C., Sanders, D.B., Mazzarella, J.M. and Soifer, B.T. 1995, ApJS, 98, 171

Fig. 1.— Images of CL 0939+4713 B at  $R$  and  $K$ , obtained using LRIS on the Keck II and NIRC on the Keck I telescopes respectively. The field is 36 " square for both filters, and the scales are identical. North is up and east to the left. CL 0939+4713 B and A are both clearly seen in the  $K$ -band image, and are visible on the  $R$ - band image. The location of CL 0939+4713 B is  $9^h 42^m 56.8^s +46^\circ 57' 48''$  (J2000).

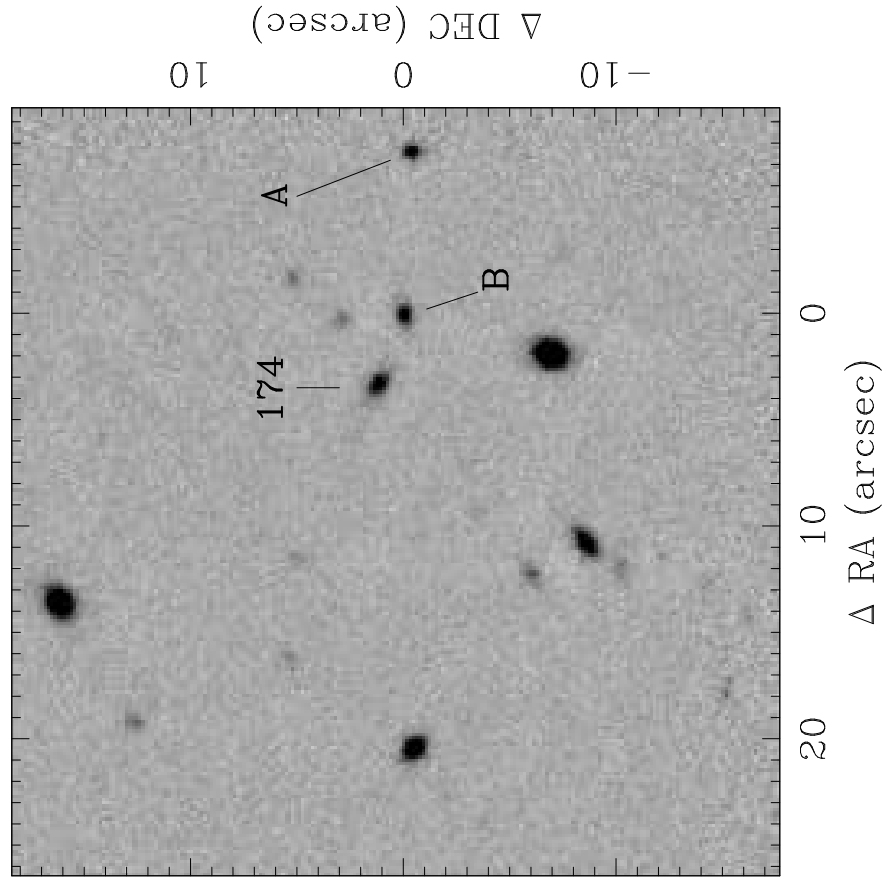
Fig. 2.— Spectrum of CL 0939+4713 B plotted as flux density  $f_\lambda$  ( $\text{Wm}^{-2}\mu\text{m}^{-1}$ ) vs. observed wavelength (in  $\mu\text{m}$ ). The hatched zones correspond the wavelength intervals that have large corrections in the division by the G star caused by low atmospheric transmission.

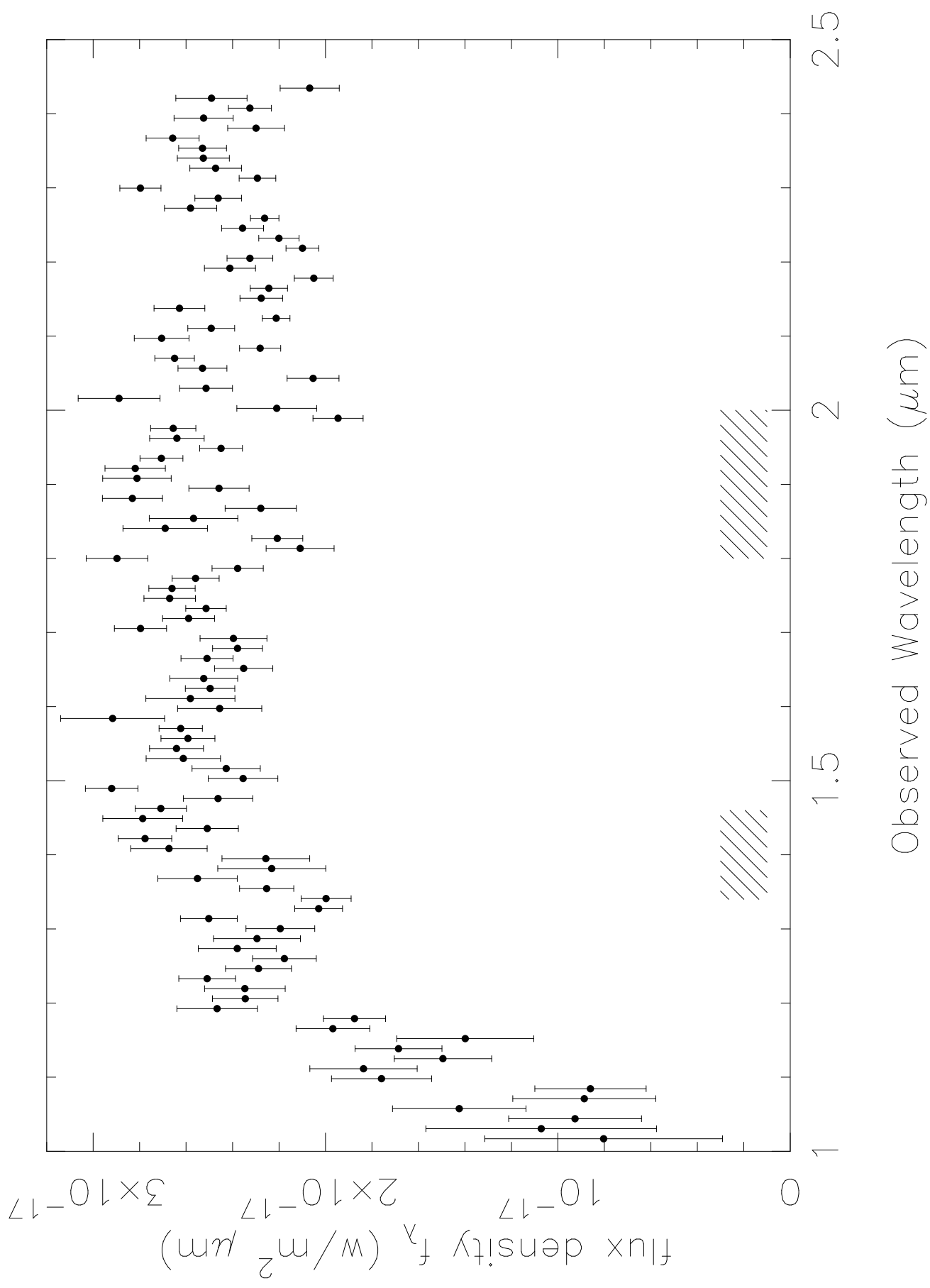
Fig. 3.— Spectrum of CL 0939+4713 B, plotted as  $\log [\text{flux}/\text{octave } \lambda f_\lambda$  ( $\text{W m}^{-2}$ )] vs. observed wavelength (in  $\mu\text{m}$ ), and compared to models of ages  $10^7, 10^8, 2.9 \times 10^8, 10^9$  and  $10^{10}\text{yr}$ . The infrared data (filled circles) are plotted at the resolution of the spectrum and the infrared fluxes have been adjusted to be consistent with the near infrared photometry. The models are for solar metal abundance, and the redshift and reddening corresponding to the values in Table 1. The models proceed from youngest to oldest from top to bottom. The  $R$  and  $I$  photometric fluxes are included as filled diamonds. Because of the widths of the band-passes, these fluxes depend on the assumed object spectrum. For the models shown, the flux per octave ranges from  $-17.48 < \log[\lambda f_\lambda(\text{Wm}^{-2})] < -17.36$  ( $I$ ) and  $-18.27 < \log[\lambda f_\lambda(\text{Wm}^{-2})] < -17.94$  ( $R$ ). The values calculated for a Bruzual and Charlot (1993, 1996) model with an age of  $2.9 \times 10^8$  yrs are plotted; the precepts outlined in the Explanatory Supplement to the IRAS Catalogs and Atlases (Joint IRAS Science Team 1989) for color corrections were followed. The effective wavelengths of the band were chosen as 0.61 and 0.81  $\mu\text{m}$ . The horizontal bars on the  $R$  and  $I$  points indicate the full widths at half peak of the filter and CCD transmission.

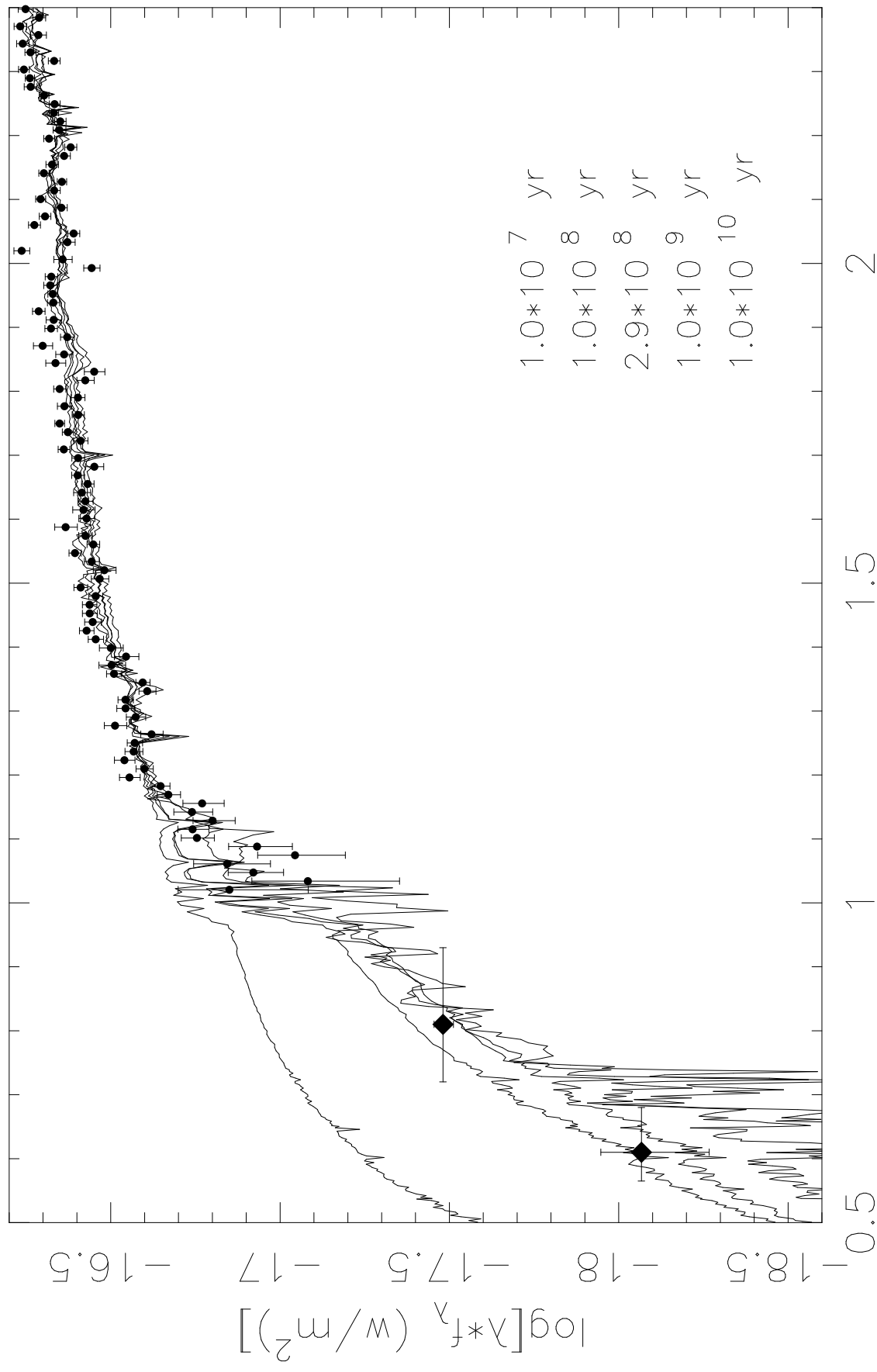
LRIS R-band image



NIRC K-band image







Observed Wavelength ( $\mu\text{m}$ )